Experimental and numerical study of tooth finishing processes contribution to gear noise

Simon Jolivet, Sabeur Mezghani, Jérôme Isselin, Mohammed El Mansori

Experimental and numerical study of tooth finishing processes contribution to gear noise

S. Jolivet [a], S. Mezghani [a], J. Isselin [a], M. El Mansori [b]

[a] Arts and Métiers ParisTech. Mechanics, Surfaces and Materials Processing (MSMP), Rue Saint Dominique, BP 508, 51006 Châlons-en-Champagne Cedex, France
[b] Arts and Métiers ParisTech. Mechanics, Surfaces and Materials Processing (MSMP), 2 Cours des Arts et Métiers, 13617 Aix-en-Provence, France

A B S T R A C T

The contribution of gear tooth flank surface micro-finish on gear noise has not yet been taken into consideration. This paper is devoted to study the simultaneous effect of tooth roughness and lubricant viscosity on automotive gear vibrations. The vibrations performances were evaluated on an instrumented test rig under both dry and wet conditions. A non-destructive replication technique coupled to 3D optical measures was used to acquire the flanks topographies, which were characterized using multiscale decomposition. A three-dimensional finite element simulation of a helical gear was performed to assess the micro-scales impact on gear noise. Numerical representative surfaces morphologies were introduced into the simulation and compared through the transmission error calculation. Results have shown gear noise dependence on tooth finishing processes.

Keywords:
Gear vibrations
Multiscale surface characterization
Dry and lubricated contact
Finishing processes

1. Introduction

The development of electric motorizations has increased the need for high quality gears in the automotive powertrain transmissions, as the combustion does not cover its noise anymore. It is known that gear meshing produces vibrations due to load variations on the teeth. Indeed, this uneven load generates excitations which are then transmitted to the environment and produce noise. Nevertheless, manufacturing and assembly defects such as profile [1,2], division [3–5] and eccentricity errors [6,7] amplify this inherent behavior by enhancing the existing excitations. To counteract this, teeth corrections such as crowning are put in place. The industrial manufacturing of gear tooth of a powertrain transmission for an automotive application involves an interrupted multistage process to meet its mechanical contact functionalities. It is a succession of several stages. First, the teeth are cut using a continuous hobbing operation. The gears are then shaved before carbonitriding. Shaving is a machining process in which the tool"s cutting edges (Fig. 1a) come scraping the tooth flanks during the meshing with the piece. It removes the fine particles under high pressure [8]. Then, carbonitriding allows the hardening of the surface, thus effectively reducing wear. Finally, the gear surfaces are shot-peened. Manufacturing errors due to these operations can then be reduced using a finishing operation after shot-peening such as power honing or grinding. Both of these are abrasive processes which use the meshing mechanics to machine the flanks. The power honing process (Fig. 1b), uses an internal gear with shafts that are not parallel to generate an increased lateral friction on the flanks and thus correct tooth surface irregularities [9]. Due to this, the load is important but balanced along the width of the teeth; it leaves high residual compressive stress [10]. Grinding (Fig. 1c) is very often used as a worming gear in order to generate friction between the abrasive surface and the workpiece. It is a process which has high cutting speed and thus induces high temperatures [11], which can lead to "grinding burns" on the flanks. The whole multi-step process produces structured surfaces which need to be characterized on the entire wavelength band.

In the automotive industry, vibratory tests are performed to select the adequate gear finishing process. However, they can quickly become time consuming and costly. Thus researchers have turned to simulation and modeling in order to overcome these limits. Nevertheless, these models take into account only geometrical deviations at the macro scale as it is required in manufacturing tooth specifications. They do not consider the finishing process and its micro-scale signature. Studies by Åkerblom [13,14] have focused on this effect without giving significant global conclusions but they showed that a higher roughness tends to increase gear noise by 1 or 2 dB. Most developed models calculate the gear transmission error, defined by Harris [15] and Welbourn [16] as the deviation between the theoretical angular position of the driven gear and its actual position. It has been shown to be the main cause of gear noise [17–19]. However, the multi-step manufacturing process can introduce micro-geometry deviations on

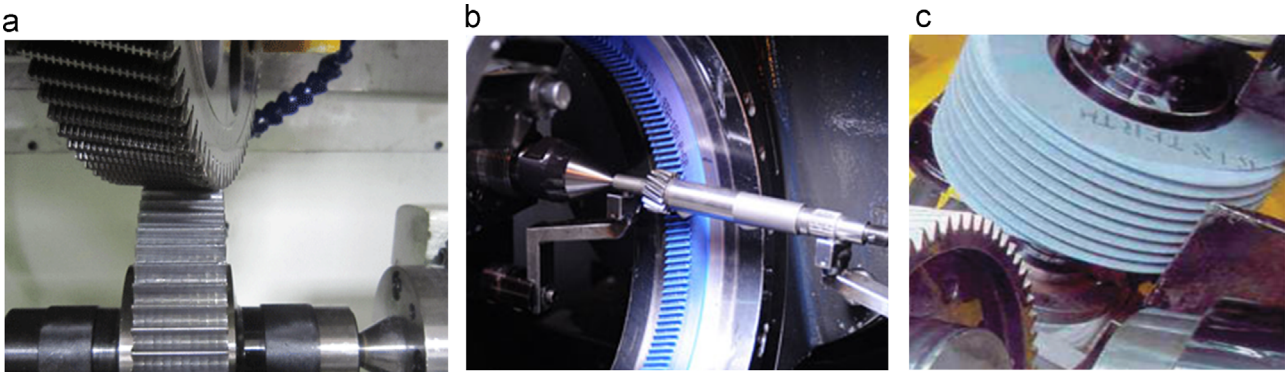

Fig. 1. Tooth flank finishing processes: (a) shaving process, (b) power honing with internal meshing and (c) grinding with worm meshing [12].

the flanks which can alter the meshing contact and influence gear noise [20].

In this paper, experimental and numerical studies were developed to study the influence of tooth finishing process on gear noise under dry and wet conditions. Three configurations are considered: not finished, finished by power honing and finished by grinding. The vibratory response of each gear as well as the topographic teeth surface modification have been used as a signature of the considered finishing process before, during and after the meshing tests. Furthermore, a finite element model of a helical gear computing transmission error has been developed. Then the relationship between the surface irregularities, the lubrication and the generated vibrations were analyzed in a wide range of wavelength from roughness to waviness.

2. Multiscale signature of each gear manufacturing step

In order to characterize the evolution of three-dimensional texture on the flank surfaces at different instants of the vibratory test, a nondestructive technique was used. Replicates of the primary shaft teeth were made with a silicone-based resin (Struers, Repliset F1) which were then measured at the primitive diameter with a white-light interferometer (WYKO 3300 NT –WLI), sampled at 515×515 points with a 3.88 μm step in both x and y directions. The form error component was removed from the acquired 3D data using least squared approximation method based on a cubic spline function.

Fig. 2 presents typical tooth surface morphology after each manufacturing steps. It is interesting to note that facets appear on the flanks after hobbing (Fig. 2a). The next step, the shaving operation, introduces oriented grooves on the surface (Fig. 2b). The carbonitriding does not significantly change the surface morphology (Fig. 2c). This figure also shows that surface topography (Fig. 2d) is very rough without the finishing step as compared to the finished surfaces. The power honing generates surfaces with curved grooves (Fig. 2e) while the grinding generates ones oriented in the helix direction (Fig. 2f). These are due to the significantly different process kinematics.

Fig. 3 gives the ISO 25178 standard parameters for each step. The arithmetic average roughness (Sa) is decreasing during the overall manufacturing processing. The roughness is very close between the two finishing processes, grinding and power honing; it is reinforced by their overlapping standard deviations. Three functional parameters from the bearing curve were considered for tooth surface characterization. The core roughness depth (Sk) is a measure of the surface with the predominant peaks and valleys removed. The Reduced Valley Depth (Svk) is a measure of the valley depth below the core roughness while the Reduced Peak Height (Spk) is a measure of the peak height above the core roughness. In the same manner as the (Sa) parameter, they tend to decrease as manufacturing advances. They also indicate that grinded surfaces tend to have higher functional peaks and less deep valleys. However the differences are not significant.

As the flanks were generated in several steps, the surfaces irregularities occur on large wavelength band. Then, multi-scale analysis based on the continuous wavelet transform was used to identify the relationship between surface irregularities and the functional finish product behavior [21–23]. Then, the surfaces were decomposed in the profile direction of the teeth, using Morlet wavelet function. The multiscale roughness spectra, called SMa, were then calculated [24,25]. It represents the arithmetic average roughness computed at each scale of the surface, and thus at each wavelength. From there, the Multiscale Process Signature (MPS) can be computed with the relative difference between the initial surface SMa and the final one:

$$MPS = \frac{SMa_{final} - SMa_{initial}}{SMa_{final}} \quad (1)$$

Fig. 4 shows the process signature of each manufacturing step, which is the relative difference of the SMa before and after the considered processing step. It demonstrates clearly that the shaving process introduces a high roughness on the facets made on the flanks by the hobbing tool (Fig. 2a). Indeed, while a representative surface after hobbing is very rough, the roughness inside these facets is very low. The carbonitriding operation dilates the surface and offers a small but significant increase of the amplitude in the waviness scales, superior to 0.2 mm. After that, the craters left by the shot peening operation largely increase the amplitude in the roughness scales, while leaving the waviness ones intact. In the end, the hard finishing operations correct the irregularities of the preceding steps at all scales. Furthermore, it can be noted that there is a difference between the two finishing processes: the grinding operation leaves higher waviness amplitudes on the flanks than the power honing step and reversely in the roughness scales. In the end, the finishing operation erases the irregularities left by the preceding steps on all scales.

3. Experimental vibratory tests on single stage gears

An instrumented low-powered vibratory testing rig for a single-stage gear was developed in order to test the gears, as shown in Fig. 5 [12]. The primary shaft is driven by a 2.4 kW asynchronous motor while a resisting load is applied by a 2.1 kW DC machine linked to a 4 kW rheostat. Both machines are assembled on silent blocs. Flexible couplings make the liaison with the electric machines to reduce the vibration transmitted to the gear.

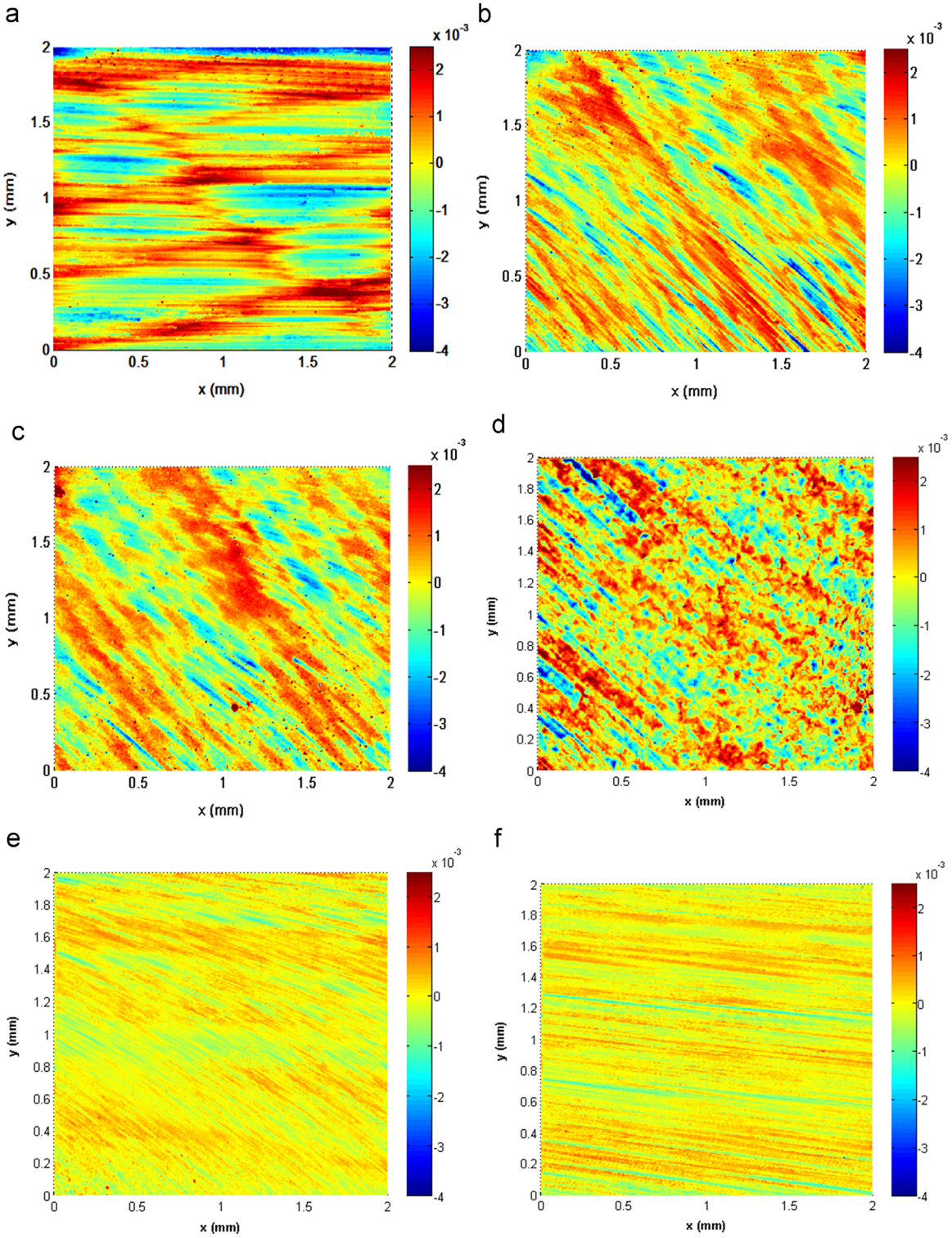

Fig. 2. 3D micro-topographies (2 mm × 2 mm) of tooth surfaces generated respectively (a) after hobbing, (b) after shaving, (c) after carbonitriding, (d) after shot peening (without hard finishing), (e) by power honing and (f) by grinding. The color scale is in millimeters. (For interpretation of the references to color in this figure legend, the reader is referred to the web version of this article.)

The gear (23 × 51 teeth) comes from an automotive powertrain transmission. Three configurations were then studied for the primary shaft. The first one uses a power honing operation, the second a grinding one and the third does not have a finishing operation. For the latter, the shaving process was slightly changed in order to maintain the same geometric and dimensional on the product. The secondary shaft was grinded and it was changed after each experimental test by a new one with identical geometric as well as surface characteristics to have the same initial conditions in each test. The teeth were manufactured so that their

macro-geometric and form parameters were maintained as close as possible. The tests lasted for two hours with a 1500 rpm speed and an 8 Nm load on the driven gear.

Dry and wet regimes using two lubricant viscosity, "Oil A" and "Oil B" are considered for each test. The oil temperature varied averagely from 20 to 33 °C during experiments. The dynamic viscosity of "Oil A" ranged from 40 to 70 centipoise while it ranged from 250 to 500 centipoise for "Oil B". Each test configuration was repeated for three times.

Every 15 minutes, gear vibrations were acquired with an accelerometer (Brüel&Kjaer, 4533-B) which was placed radially to the rotation of the gear, at the top of the assembly as shown in Fig. 2. The signal was conditioned before it being recorded (Brüel&Kjaer, conditioning amplifier 1704-A-002). The vibration acquisition was averaged on 128 signals of 1.6 s each and sampled at 5120 Hz.

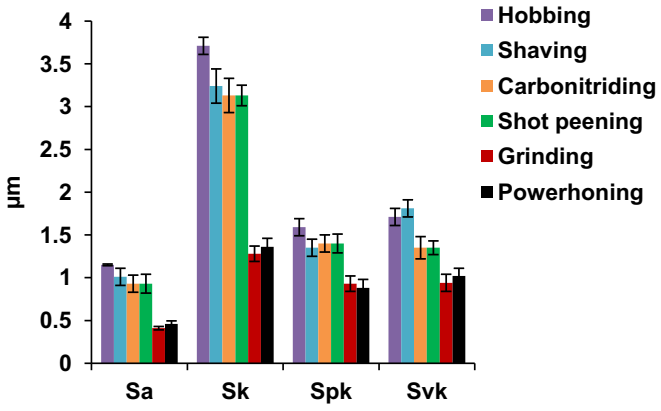

Fig. 3. ISO 25178 standard surface parameters of gear tooth flanks after each manufacturing step.

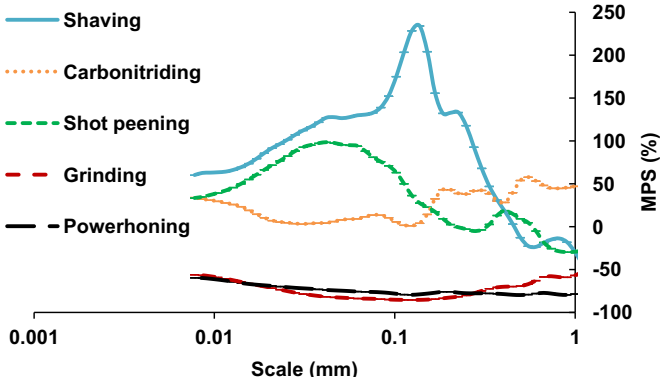

Fig. 4. Multiscale Process Signatures (MPS) of each manufacturing step.

4. Numerical simulation of transmission error of helical gear

A finite element elastic model has also been developed to simulate the impact of various surface parameters on gear noise, and more precisely on transmission error. The gear geometry as well as the experimental conditions (rotation speed and load) are respectively the same as the experimental ones: 23×51 teeth, 1500 rpm on the driving gear, 8 Nm on the driven gear. The characteristics of the gear pair are given in Table 1. Abaqus (SIMULIA, Dassault Systèmes) software was used for these dry contact simulations. The mesh has the particularity to be very refined on the surface of the teeth, where we used C3D8R quadratic elements of 30 µm × 30 µm size, which were then tied to the rest of the body by a tie constraint. For the other parts of the gear's body, C3D10 were used in an adaptive mesh (Fig. 6). This mesh permitted to introduce roughness error directly on the teeth surfaces by vertically moving the nodes along the direction normal to the surface [26].

The transmission error was calculated from the angle deviation between the driving and driven gears, during the meshing of the central pair of teeth which has the most refined mesh. It was then extrapolated on a full primary shaft rotation and studied in the frequency space through Fourier transform.

5. Results and discussion

5.1. Experimental tests on the influence of ISO surface parameters on gear noise in dry conditions

The acquired vibration signals from the experimental tests were decomposed using Fast Fourier Transform (FFT). Then, the average amplitude of the first three meshing harmonics, called "L_m" was computed. As the primary shaft has 23 teeth and it was rotating at 1500 rpm (25 Hz) during the tests, the meshing orders considered were thus 575; 1150 and 1725 Hz.

From these tests, the influence of two surface parameters on the Lm value was studied: the roughness amplitude through the mean square roughness S_q defined in the ISO 25178 standard and the roughness scale through the autocorrelation length S_{al}. The values of these parameters were determined from the direct measurements on the tooth flanks as shown in Table 2.

The results of their influence on gear noise, and more precisely on the Lm value at 120 minutes, are given in Fig. 7. On one hand, we can note the influence of surface roughness on the average amplitude of the meshing harmonics. Indeed, there a clear positive

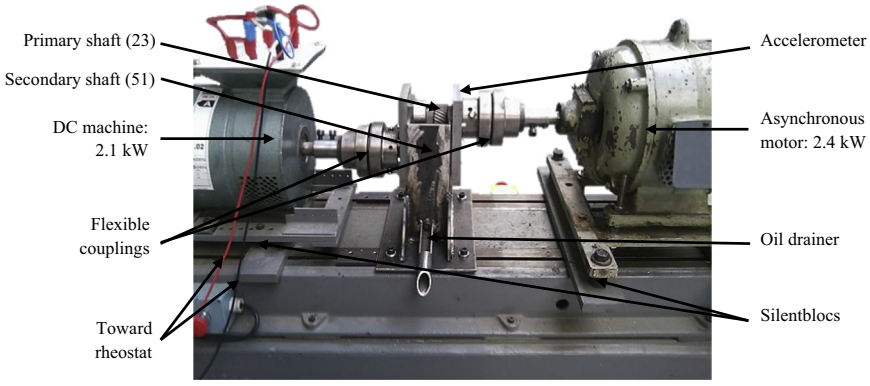

Fig. 5. Instrumented low-powered vibratory test rig for single-stage gear.

Table 1
Gear and material characteristics.

Gear pair geometry	Values	Material parameters	Values
Modulus	1.85 mm	Material	Steel
Pressure angle	20°	Young's Modulus	210 GPa
Center distance	75 mm	Density	7800 kg · m^{-3}
Helix angle	25°		
Active facewidth	24 mm		
Driving gear geometry	**Values**	**Driven gear geometry**	**Values**
Teeth number	23	Teeth number	51
Root diameter	43 mm	Root diameter	96 mm
Tip diameter	53 mm	Tip diameter	107 mm

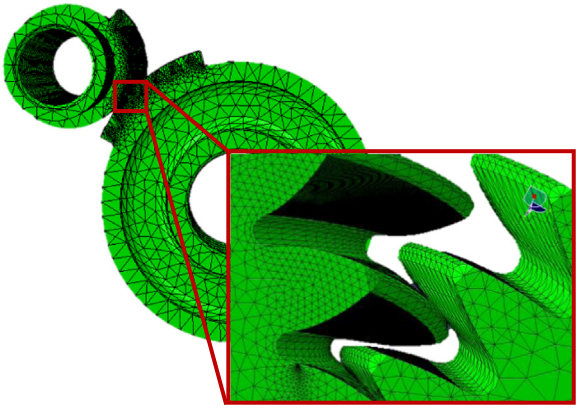

Fig. 6. Mesh of the helical gears of the finite element model.

Table 2
Auto correlation length in the profile and helix directions as well as quadratic roughness for each of the three studied configurations.

	S_{al} in the profile direction (μm)	S_{al} in the helix direction (μm)	Quadratic roughness (μm)
Grinding	48.5	122.3	0.53
Power honing	17.5	25.2	0.64
No finishing	21.4	17.5	1.02

linear relation between the two (Fig. 7a). On the other hand, the impact of the autocorrelation length is more difficult to interpret (Fig. 7b). There is no clear trend linking the two, be it in the profile or the helix direction. Nevertheless, it is interesting to note that above 50 μm the increase in autocorrelation length does not impact gear noise anymore. In the end, this lets us conclude that the roughness amplitude has a more impactful effect on gear noise in dry conditions. This can be explained by the fact that the increase of roughness amplitude leads to the increase of noise induced by friction during the contact that occurs between surfaces asperities in this regim.

5.2. Numerical simulation on the influence of ISO surface parameters on gear noise in dry conditions

Virtual texturing can be used to generate surfaces possessing chosen distinct characteristics and sampling. In order to better understand the impact of the surface on the meshing vibrations, virtual surfaces with Gaussian distributions and characteristics based of the ones measured directly on the studied flanks were generated (Fig. 8).These topographies were then integrated in the simulation model.

The results obtained after simulation are given in Fig. 9. It gives the mean amplitude of the first three meshing harmonics as a function of the studied surface parameters: it is the same parameter

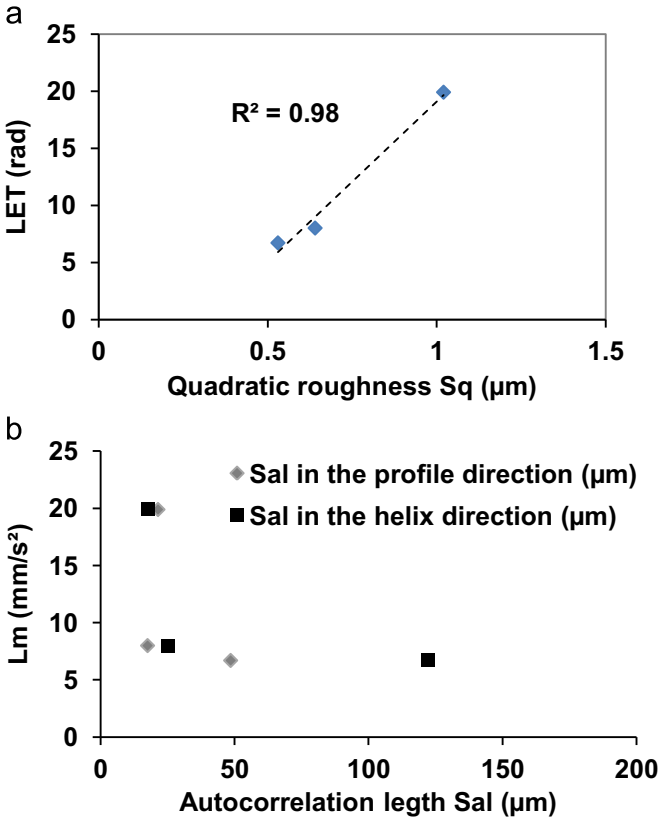

Fig. 7. Average amplitude of the vibrations first three meshing harmonics as a function of (a) quadratic roughness and (b) autocorrelation length.

used experimentally, by calculated on the transmission error signal. We can clearly see in Fig. 9a that the roughness amplitude has a very negative impact on transmission error. Indeed, it increases linearly with the quadratic roughness. This trend is very close to the experimental one as shown earlier. On the contrary, the Fig. 9b indicates that a higher surface scale decreases the transmission error amplitude, but is not as significant as roughness amplitude. When compared to the experimental results (Fig. 7b), this trend is quite different and could be explained by the fact that the surfaces do not have the same morphology.

5.3. Experimental tests on the influence tooth finishing process on gear vibrations in dry conditions

As mentioned before, the experimental tests were run over two hours. The Fig. 10 shows the L_m parameter as a function of the meshing time, for all three studied configurations. The most obvious observation is that the vibration level is higher when the flanks are not finished. Lm is about three times more important at every time step. The difference in global roughness, represented by the Sq parameter in Table 2, between the configurations with and without finishing can explain this behavior: there is more than a factor of two between the configurations. However the variations of Lm cannot be explained with these parameters only. Indeed, a transitional regime in terms of vibrations can be observed during the first 45 min.

In this regime, the vibration amplitudes for the power honing flanks finish and those without finishing increase before decreasing and stabilizing. It can be explained through the computation of the Multiscale Meshing Signature (MMS) between these aforementioned time steps. It is the relative difference between the initial SMa and the one at the considered time step. The results for the configuration without finishing and with power honing are

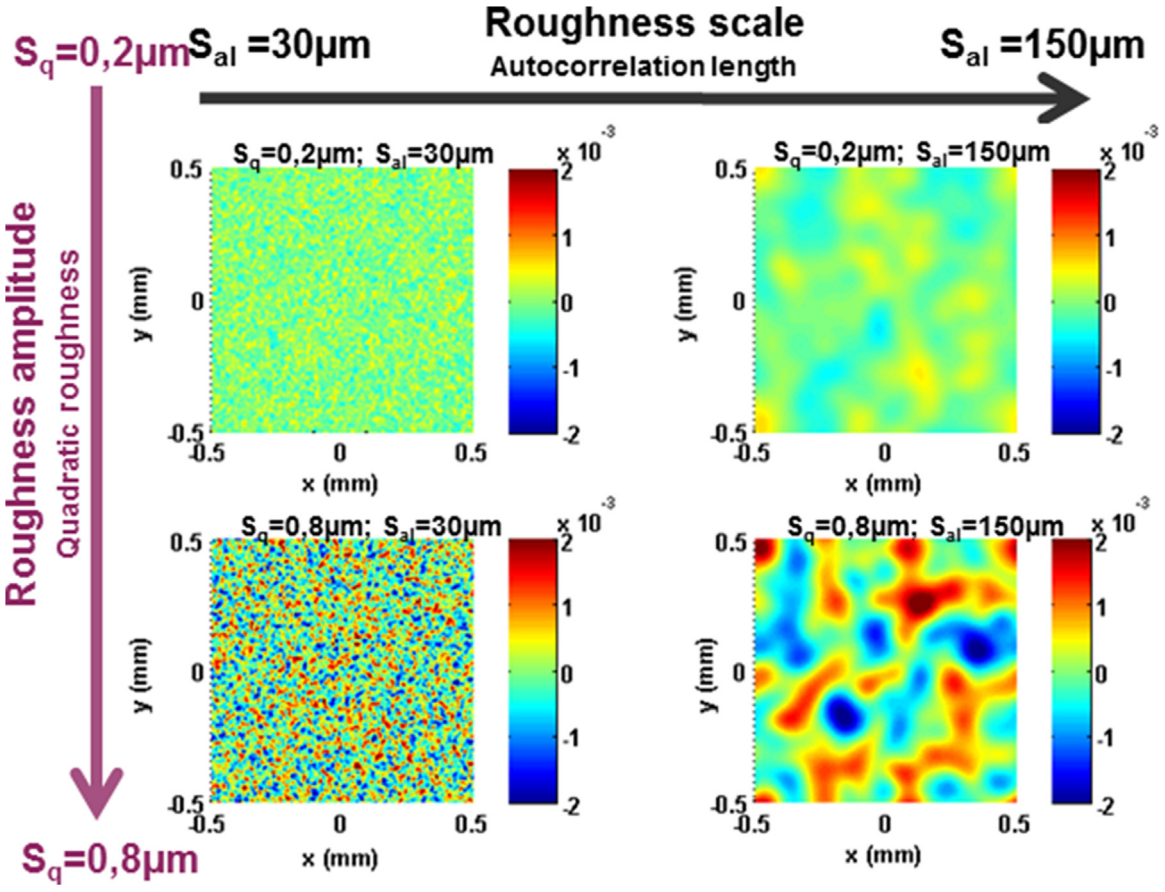

Fig. 8. Examples of virtual surfaces integrated in the numerical simulations.

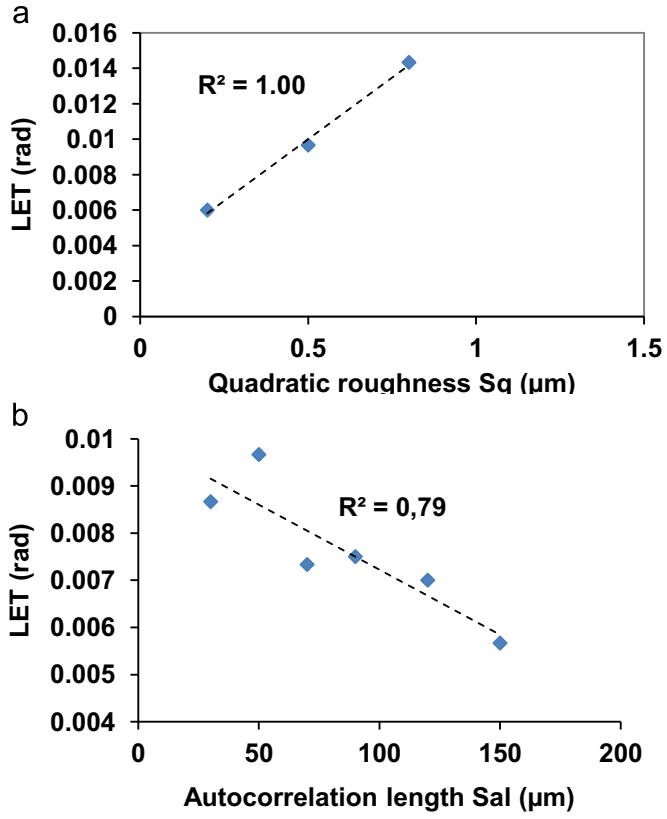

Fig. 9. Average amplitude of the transmission error's first three meshing harmonics as a function of (a) quadratic roughness and (b) autocorrelation length.

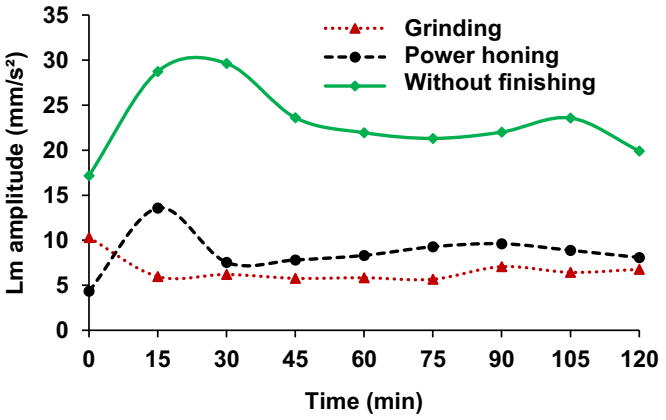

Fig. 10. Average amplitude of the vibrations' first three meshing harmonics as a function of meshing time for all three studied configurations.

given in Fig. 11. Despite the modifications in the roughness scale, a common behavior can be highlighted in the waviness scale. Indeed, above 0.2 mm for the configuration without finishing and above 0.4 mm for the power honing, there is an increase in surface amplitude which is not negligible. These changes in the mesoscales, which are adaptation of the surface to the meshing, could explain the increase of vibration amplitude for these two configurations. As for the grinded samples, we were unable to investigate the vibrations values between the 0 and 15 min time steps.

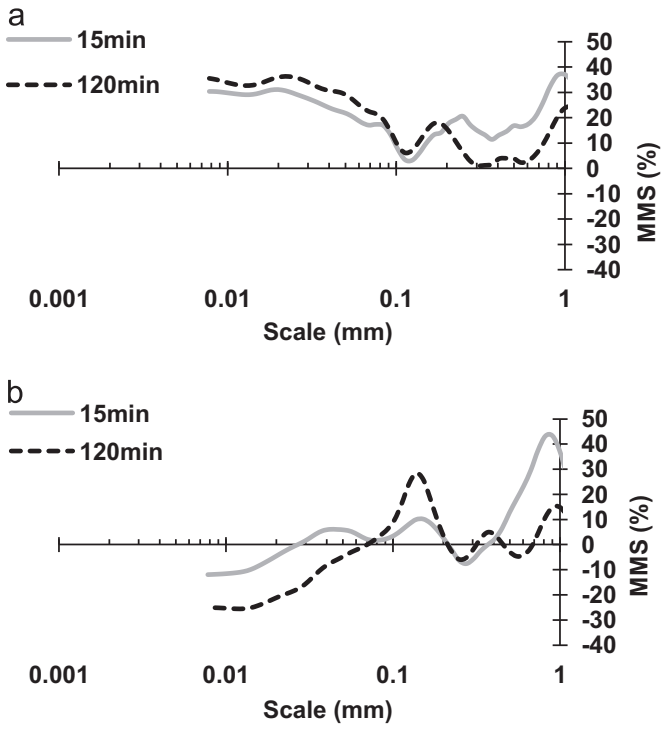

Fig. 11. Multiscale Meshing Signature for the configurations (a) without finishing and (b) with power honing.

5.4. *Experimental tests on the influence tooth finishing process on gear vibrations in lubricated conditions*

In order to quantify more precisely the effect of each factor (lubrication, roughness, waviness, time) on the average of the vibratory amplitude of the first three meshing harmonics, a variance analysis by linear regression on the L_m parameter was considered. A type III sum of squares was chosen in order to test the main effects as well as their interactions. The validation of the model was evaluated by the calculation of the correlation coefficient R^2 [27]. It is a reel number between zero and one: a higher value indicates a model closer to the data. The Fisher test was used to quantify the significativity of each factor α by the following formula [28]:

$$\mathbf{F(\alpha)} = \frac{\mathbf{MS_{reg}(\alpha)}}{\mathbf{MS_r}} \tag{2}$$

Where MS_{reg} is the mean of the squares due to the regression and MS_r the mean of the squares of the residue. To quantify the C contribution of each factor to the parameter L_m, the quotient of the contribution C of each factor α was calculated with the Fisher test with a R^2 trust [29,30]. It is defined by:

$$\mathbf{C(\alpha)} = \frac{\mathbf{F(\alpha)}}{\sum_{\alpha}\mathbf{F(\alpha)}} \times \mathbf{R^2} \tag{3}$$

Then:

$$\sum_{\alpha}\mathbf{C(\alpha)} = \mathbf{R^2} \tag{4}$$

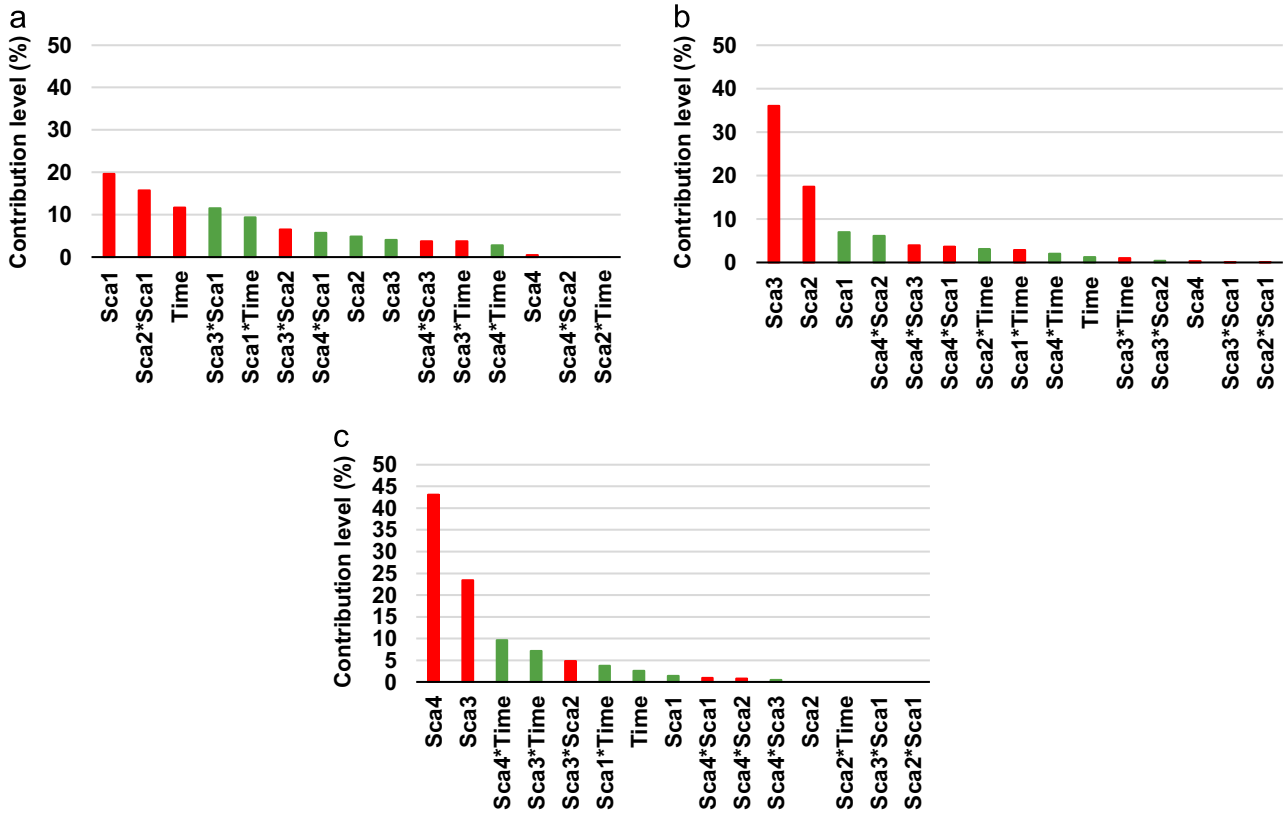

Fig. 12. Contribution percentage in each of lubrication conditions: (a) dry meshing; (b) oil A (fluid); (c) oil B (viscuous). Red indicates a negative contribution to gear vibration (meaning higher vibration amplitude) and green a positive contribution. (For interpretation of the references to color in this figure legend, the reader is referred to the web version of this article.)

This analysis was done with the software XLSTAT (Microsoft). As variables of the models, the following parameters were considered:

- Time: in minutes;
- Sca1: average of SMa for the scales from 0 to 0.025 mm;
- Sca2: average of SMa for the scales from 0.025 to 0.25 mm;
- Sca3: average of SMa for the scales from 0.25 to 0.75 mm;
- Sca4: average of SMa for the scales from 0.75 to 1.5 mm.

The results giving the percentage contribution are in Fig. 12. In dry meshing, Fig. 12a, we can note that the roughness scales from 0 to 0.025 mm have the largest impact on gear vibrations as their contribution are around 20%. The interaction of these scales with the ones between 0.025 and 0.25 mm are also important with more than 15% contribution. This result corroborates what we have shown both experimentally and numerically. When lubricant is introduced, Fig. 12b, there is a shift of the impactful scales toward waviness, as the major factor is the scales between 0.25 and 0.75 mm. The roughness factor, Sca2, stays influent. When the lubricant viscosity is increased, Fig. 12c, the shift is even more prominent as the main factors are Sca4 with more than 40% contribution and Sca3 with around 25%. Thus as viscosity increases, the influent scales on gear vibrations shift from microroughness toward waviness. This can be explained by the presence of a thicker oil film between the teeth, reducing the number of asperities in contact and leading to the increase the spacing interval between different contact area and therefore enhancing the impact of higher surface scales.

6. Conclusions

This study highlighted a methodology to developed and quantify the contribution of each surface scale on the gear noise, permitted by the use of multiscale surface decomposition based on wavelet transform. The results obtained for dry meshing experimentally and numerically showed that the surface, and more precisely the microroughness, had a large impact on gear vibrations, indicating that finishing processes were influent. The subsequent experimental tests in wet conditions have shown that the surface scales are still very influent and thus need to be included in future studies. Indeed, the lubricant and its viscosity shifted the influent scales toward waviness. Perspectives include the integration of lubrication in the simulations in order to develop a powerful predictive tool to optimize the choice of finishing process in gear manufacturing.

Acknowledgments

Funding for this research was provided by Renault SAS. The calculations would not have been possible without the support of the HPC Center of Champagne-Ardenne ROMEO.

References

[1] Munro RG. Gear Transmission Error. AGMA Aerospace Gearing Commitee Meeting, vol 10. Portsmouth; 1967.
[2] Mark WD. Analysis of the vibratory excitation of gear systems: basic theory. J Acoust Soc Am 1978;63:1409–30.
[3] Mark WD. Gear noise origins. In: Proceedins of the AGARD conference (propulsion energy panel symposium). Lisbonne; 1984, p. 1–14.
[4] Salzer MLW, Smith JD, Welbourn DB. Simulation of noise from gears when varying design and manufacturing parameter. Paris: World Congress on Gearing; 1977.
[5] Welbourn DB. Gear noise spectra – a rational explanation. In: Proceedings of the ASME international power transmission and gearing conference. Chicago (US); 1977.
[6] Welbourn DB. Gears errors and their resultant noise spectra. Gearing 1970;184:131–9.
[7] Munro RG. A review of the theory and measurement of gear transmission error. In: Proceedings of the 1st international conference on gearbox noise and vibration. Cambridge; 1991, p. 3–10.
[8] Henriot G. Taillage et finition des engrenages. Tech L'Ingénieur 1984.
[9] Mehta DT, Rathi MG. A Review On Internal Gear Honing. Int J Eng Res Technol 2013;2:973–83.
[10] Karpuschewski B, Knoche H-J, Hipke M. Gear finishing by abrasive processes. CIRP Ann – Manuf Technol 2008;57:621–40. http://dx.doi.org/10.1016/j.cirp.2008.09.002.
[11] Brinksmeier E. Giwerzew a. Hard gear finishing viewed as a process of abrasive wear. Wear 2005;258:62–9. http://dx.doi.org/10.1016/j.wear.2004.09.032.
[12] Jolivet S, Mezghani S, Isselin J, Giraudeau A, El Mansori M, Zahouani H. Evaluation of Tooth Surface Micro-Finishing on Gear Noise. Key Eng Mater 2015;651–653:498–503. http://dx.doi.org/10.4028/www.scientific.net/KEM.651-653.498.
[13] Åkerblom M. Gear noise and vibration – a literature survey. Stockholm; 2001.
[14] Åkerblom M, Pärssinen M. A study of gear noise and vibration; 2002.
[15] Harris SL. Dynamic Loads on the Teeth of Spur Gears. Proc Inst Mech Eng 1958:87–112.
[16] Welbourn DB. Fundamental knowledge of gear noise – a survey. In: Proceedings of the conference on noise vibration engines transmission. Cranfield; 1979, p. 9–29.
[17] Davoli P, Gorla C, Rossa F, Rossi F. Transmission error and noise excitation of spur gears. In: Proceedings of the 10th ASME International Power Transmission Gearing Conference. Las Vegas; 2007.
[18] Podzharov E, Syromyatnikov V, Ponce Navarro JP, Navarro RP. Static and dynamic transmissin error in spur gears. Open Ind Manuf Eng J 2008;1:37–41. http://dx.doi.org/10.2174/1874152500801010037.
[19] Henriksson M. On noise generation and dynamic transmission error of gears [Doctoral thesis]. Stockholm, Sweden: KTH University; 2009.
[20] Bihr J, Heider M, Otto M, Stahl K, Kume T, Kato M. Gear noise prediction in automotive transmissions. In: Proceedings of the international gear conference; 2014, p. 457–65.
[21] Mezghani S, Mansori M, El, Massaq A, Ghidossi P. Correlation between surface topography and tribological mechanisms of the belt-finishing process using multiscale finishing process signature. Comptes Rendus Méc 2008;336:794–9. http://dx.doi.org/10.1016/j.crme.2008.09.002.
[22] Jolivet S, Mezghani S, Mansori M, El, Zahouani H. Gear noise behavior induced by their topological quality. Surf Topogr Metrol Prop 2013;2:014008. http://dx.doi.org/10.1088/2051-672X/2/1/014008.
[23] Jolivet S, Mezghani S, El M, Jourdain B. Dependence of tooth flank finishing on powertrain gear noise. J Manuf Syst 2015;37:467–71. http://dx.doi.org/10.1016/j.jmsy.2014.11.006.
[24] Zahouani H, Mezghani S, Vargiolu R, Dursapt M. Identification of manufacturing signature by 2D wavelet decomposition. Wear 2008;264:480–5. http://dx.doi.org/10.1016/j.wear.2006.08.047.
[25] El Mansori M, Mezghani S, Sabri L, Zahouani H. On the concept of process signature in analysis of multistage surface formation. Surf Eng 2010;26:216–23.
[26] Thompson MK, Thompson JM. Considerations for the incorporation of measured surfaces in finite element models. Scanning 2010;32:183–98. http://dx.doi.org/10.1002/sca.20180.
[27] Wold S, Sjöström M, Eriksson L. PLS-regression: a basic tool of chemometrics. Chemom Intell Lab Syst 2001;58:109–30. http://dx.doi.org/10.1016/S0169-7439(01)00155-1.
[28] Massart DL, Vandeginste BG, Buydens LMC, De Jong S, Lewi P, Smeyers-Verbeke J. Handbook of chemometrics and qualimetrics: part A. . Amsterdam: Elsevier; http://dx.doi.org/10.1016/S0922-3487(97)80056-1.
[29] Davim JP, Reis P. Damage and dimensional precision on milling carbon fiber-reinforced plastics using design experiments. J Mater Process Technol 2005;160:160–7. http://dx.doi.org/10.1016/j.jmatprotec.2004.06.003.
[30] Ryan TP. Modern engineering statistics. Acworth, Georgia: Wiley. Wiley-Interscience; 2007.